ELSEVIER

Thermochimica Acta 285 (1996) 325–336

thermochimica acta

Thermal decomposition of hexahydrated nickel iron citrate

N.S. Gajbhiye*, Seema Prasad

Department of Chemistry, Indian Institute of Technology, Kanpur 208016 U.P., India

Received 30 August 1995; accepted 10 February 1996

Abstract

The citrate precursor method has been used to synthesise ultrafine $NiFe_2O_4$. The citrate precursor, $Ni_3Fe_6O_4(C_6H_6O_7)_8 \cdot 6H_2O$, was isolated by thermal heat treatment at around 100°C. Thermal decomposition of the hydrated precursor was investigated by TG, DTA and DTG techniques, and gas and chemical analyases. The citrate precursor, on decomposition in air, yields pure and stoichiometric $NiFe_2O_4$. The decomposition consists of three major steps. The dehydration step of the citrate precursor is overlapped by the formation of an acetonedicarboxylate complex. The citrate groups are completely destroyed in the temperature range 200–320°C resulting in the formation of $NiFe_2O_4$ with the evolution of acetone and CO_2 gas. The free CO_2 gas is trapped in the lattice and is released above 320°C. The ultrafine $NiFe_2O_4$ particles have been observed as clusters having a crystallite size of 5.93 nm and a surface area of 120.0 $m^2 g^{-1}$. The citrate precursor and decomposed products were characterized by IR, NMR, XRD, SEM and surface area measurements.

Keywords: Citrate; Ferrite; Precursor; Thermal Decomposition; Ultrafine

1. Introduction

Magnetism of fine particles is of considerable interest from the points of view of basic scientific understanding and technological applications. The preparation of spinel ferrites has been technologically important to the microwave industries for a long time. In the past ten years or so the production of ferrites with small particle characteristics has been important for high speed digital tape or disk recording [1] and has a future application as a repulsive suspension for use in levitated railway systems [2]. This has

* Corresponding author. Tel: 0325 296/0325 329; Fax: 512 250260/250007.

PII S0040-6031(96)02906-1

prompted the development of various chemical methods which include hydrothermal, co-precipitation, freeze drying, spray drying and sol–gel for the preparation of stoichiometric and chemically pure spinel ferrites [3–8]. In particular, the citrate precursor process has been shown to have great potential in the preparation of rare earth iron garnets [9,10].

No studies are available on the thermal decomposition of nickel iron citrate precursor. The present investigation deals with the preparation, characterization and mode of thermal decomposition of nickel iron citrate hexahydrate precursor, leading to the formation of chemically pure and stoichiometric nickel ferrite powder.

2. Experimental

2.1. Reagents

The reagents [$Ni(NO_3)_2 \cdot 6H_2O$ and citric acid] used were AnalaR grade from S.d. fine Chem, Boisar, India. $Fe(NO_3)_3 \cdot 9H_2O$ used was GR grade from Loba Chemie, Bombay, India.

2.2. Preparation

70 mL, 0.2 M, nickel nitrate and 85 mL, 0.2 M, ferric nitrate were mixed with 200 mL, 0.2 M citric acid, i.e. in the molar ratio of Ni:Fe: citric acid = 1:2:2.7 The resultant homogeneous solution was heated under reflux for 15 h at 90°C in a 1-L capacity round-bottomed flask. Finally the solution was slowly evaporated on a water bath to form a viscous liquid which was later transferred to a petri dish. Further drying was carried out at 100°C in an oven for 5 h to remove adsorbed water. During the process of drying the gel swells into a fluffy mass which eventually breaks into brittle flakes. The degree of hydration, i.e. adsorbed water molecules, varied from 4 to 12 per mol.

2.3. Analysis

Nickel was estimated gravimetrically with 1% ethanolic dimethyl glyoxime and weighed as nickel dimethyl glyoximate [11]. Iron was also estimated gravimetrically with 5% cupferron and subsequently weighed as Fe(III) oxide [12]. Chemical analysis by atomic absorption spectroscopy was performed with a model spectra AA-10, Varian, USA. The results from both analyses agreed well for the precursor, intermediates and end products. The citrate content of the precursor was estimated using Karpov's method in which 2 mL of citrate precursor solution was mixed with 25 mL 0.1 N $K_2Cr_2O_7$ and 5 mL conc. H_2SO_4. The solution was heated gently and excess dichromate was titrated against 0.1 N solution of Mohr's salt using 3 to 4 drops of 0.1% phenylanthranilic acid as indicator. The end point is the change of red–violet to a green colour [13]. The qualitative analysis of acetone was performed using filter paper moistened with *o*-nitrobenzaldehyde in 2 N sodium hydroxide. During decomposition

of the citrate precursor evolved acetone turns the paper bluish green. The presence of acetone was also detected by the Iodoform test and the acetone–2,4-Dinitrophenylhydrazone test. This was further confirmed by ^{1}H NMR spectral analysis using a Jeol-PMX-60 S1, Japan [14]. Quantitative analysis of acetone was performed by titrating excess acidified 0.1 N iodine solution against 0.1 N $Na_2S_2O_3$ solution in the presence of 1 N NaOH. A Perkin–Elmer 240 C elemental analyser was used to analyse the evolved gases. Thermal analyses of the citrate precursor were performed up to 1000°C with a Linseis model L-81/042 derivatiograph which records TGA and DTA simultaneously. Samples (60 mg) were placed in a platinum crucible, ignited alumina was used as the reference meterial with the heating rate of 10° min^{-1} and 5° min^{-1}. The thermal analyses were carried out in static air. Some thermoanalytical curves were recorded on Perkin–Elmer TG S2/TADS 3600 and Shimadzu DTA-50, differential thermal analysers at temperatures up to 700°C with heating rates of 10° min^{-1} and 5° min^{-1}.

X-ray diffractograms were recorded using a Rich Seifert Isodebyflex X-ray unit model 2002 with CuK_α Radiation and Ni filter. IR spectra were recorded with a Perkin–Elmer model 377 IR spectrophotometer using sample in the form of KBr pellets. Surface area measurements of the residue were obtained by the single point BET method with a Quantachrome Quantasorb sorption system model QS-7 using nitrogen gas as the adsorber.

3. Results

Wet chemical analysis of the nickel iron citrate precursor gave: Ni = 8.0%, Fe = 15.2%, H_2O = 4.9%, citrate = 71.9% which agreed well with the values calculated for $Ni_3Fe_6O_4(C_6H_6O_7)_8 \cdot 6H_2O$, Ni = 7.9%, Fe = 15.2%, H_2O = 4.9%, citrate = 71.8%. The precursor adsorbs water depending on the humidity of the atmosphere. It was amorphous to X-rays. The IR spectra of nickel iron citrate precursor, citric acid and ferric nitrate were analysed; the results are shown in Table 1, which shows that the citrate precursor has all the common bands of the citric acid. There are some bands that differ in intensity and are broad in nature, which indicates the formation of hydrated citrate precursor. The broad bands in the region 3600–3000 cm^{-1} and around 1610 cm^{-1} could be due to the stretching and bending modes of water molecules because the intensity of these absorptions decreases and disappears with the heat-treatment temperature. However, the broad band in the region 3429 cm^{-1} and the small shoulder at 1700 cm^{-1} could be attributed to the free hydroxyl and carboxylate group of nickel iron citrate. The broad and the unresolved bands at 1570 and 1400 cm^{-1} are characteristics of the completely ionised carboxyl group with equalised CO bands. No bands were observed for free citric acid (1700 cm^{-1}, vs) or ionic nitrate (1385 cm^{-1}) impurities [15]. These studies indicate that citrate groups coordinate to the Fe and Ni metal through carboxylate groups leaving free HO–C(–)–COOH groups.

Table 1
IR spectral frequency assignments for citric acid, ferric nitrate, precursor and different heat-treated products [a]

Citric acid	Ferric nitrate	Precursor	Heat treatment temperature/°C					Assignments
			140	160	200	280	320	
3300s	3700–3000vs	3700–3000vs	3700–3000vs	3700–3000w	3700–3000w	–	–	ν OH water
3450sh	–	3450sh	3450sh	–	–	–	–	ν OH hydroxyl
2900–2800s	–	2900–2800w	2900–2800w	2900–2800w	–	–	–	ν CH
–	–	–	–	–	–	2320w	2320w	ν CO_2
1700vs	–	1700vwsh	1700vwsh	1700vwsh	–	–	–	ν asymC = O
1620w	1610s	1610w	1610w	–	–	–	–	δ HOH
–	–	1570vs–	1570vs	1570s	1570vw	–	–	ν asymCOO
1430,1395	–	1400vs	1400vs	1400vs	1400vw	–	–	ν symCOO
1355s								
–	1361vs	–	–	–	–	–	–	ν_3 NO_3^-
1240–1190s	–	1270wsh	1270wsh	–	–	–	–	ν symCO
1080–1055s	–	1080br	1080br	1080br	–	–	–	ν st C–O
940–900sh	–	–	–	–	–	–	–	Citrate
–	835m	–	–	–	–	–	–	ν_2 NO_3^-
780sh	–	–	–	–	–	–	–	Citrate
600,650sh	–	–	–	–	–	–	–	Citrate
–	–	–	–	–	–	587w	587m	ν_1 $NiFe_2O_4$
–	–	–	–	–	–	396w	396m	ν_2 $NiFe_2O_4$

[a] s, strong; vs, very strong; sh, sharp; m, medium; w, weak; br, broad.

3.1. Thermal decomposition of the citrate precursor

TG, DTG, and DTA curves recorded in static air at 5° min^{-1} and 10° min^{-1} and are shown in Figs. 1 and 2 respectively. It can be seen that one-to-one correlation exists between these thermoanalytical curves indicating that the thermal effects are accompanied by weight loss. There are three major steps in the decomposition process: dehydration, decomposition of the anhydrous precursor to acetonedicarboxylate complex and decomposition of acetonedicarboxylate complex to nickel ferrite. There are two endothermic peaks corresponding to the dehydration of the citrate precursor. After dehydration there are two exothermic peaks corresponding to citrate decomposition followed by nickel ferrite formation. However steps 2 and 3 appeared as a simultaneous and /or single step process when the heating rate was 10° min^{-1} (Fig. 2). The complete data of the observed weight loss and the corresponding temperature ranges are given in Table 2.

3.2. Dehydration of the citrate precursor

As mentioned earlier, apart from the six coordinated water molecules the amount of excess water depends on the atmospheric humidity; the amount varies from 4–10%. The extra water can be removed by heating the citrate precursor at 100°C which is shown by the endotherm between 85 and 100°C. Dehydration of the citrate precursor takes place between 120 and 160°C with a maximum around 140°C, as shown by the second endotherm in Figs. 1 and 2. The thermoanalytical curves show weight loss of

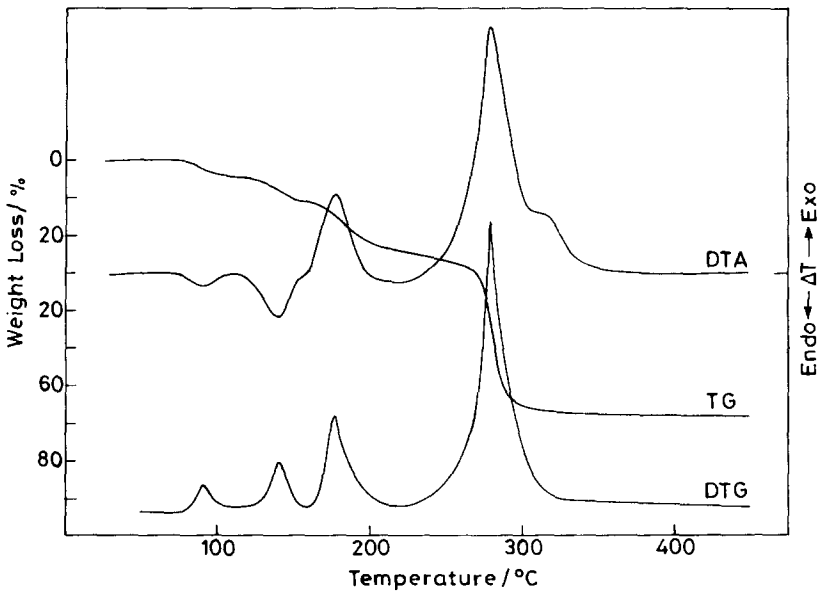

Fig. 1. TG, DTG and DTA recorded at 5° min^{-1} for nickel iron citrate precursor.

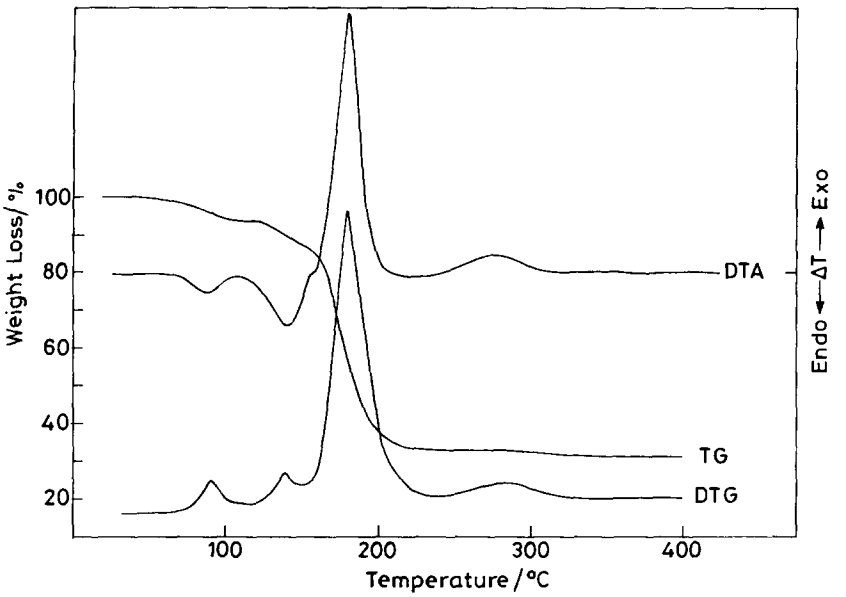

Fig. 2. TG, DTG and DTA recorded at 10° min^{-1} for nickel iron citrate precursor.

Table 2
Weight loss in decomposition steps of $Ni_3Fe_6O_4(C_6H_6O_7)_8 \cdot 6H_2O$ recorded with varying heating rate

Steps	Temp. range/°C	Heating rate = 5° min^{-1}		Observed static wt. loss / %	Heating rate = 10° min^{-1} Observed wt. loss/%
		Observed wt. loss/%	Calculated wt. loss/%		
1.	<100	4–10.0	–	9.5	4.5
2.	100–160	4.9	4.9	5.2	4.8
3.	160–200	10.7	10.2	49.1	49.3
4.	200–320	45.9	47.0	13.6	13.9
5.	>320	6.5	6.0	–	–

4.9% and 4.9%, respectively, corresponding to the loss of $6H_2O$ per mol in the citrate precursor. The temperature range mentioned above is valid only at a pressure of one atmosphere. The chemical analyses of anhydrous nickel iron citrate precursor gave Ni = 9.1%, Fe = 17.1%, citrate = 70.6%, which agreed with the theoretical values for $Ni_3Fe_6O_4(C_6H_6O_7)_8$; Ni = 8.4%, Fe = 16.0%, citrate = 72.5%.

3.3. Decomposition of the anhydrous precursor

Thermal decomposition of the anhydrous nickel iron citrate was found to be the most important and at the same time most complex stage of decomposition. The citrate precursor is probably converted to acetonedicarboxylate complex. This process is

found to be exothermic in air (Fig. 1) and large amounts of gases are evolved spontaneously. The decomposition of the anhydrous citrate precursor started around 160°C and was accompanied by the evolution of CO gas. The weight loss of 10.7% was recorded up to 200°C in air as compared with the calculated value of 10.2% for the formation of acetonedicarboxylate complex $Ni_3Fe_6O_4(C_5H_6O_6)_8$ as shown in Table 2. There is evolution of a large amount of CO gas which on combustion, i.e. secondary reaction of carbon monoxide, makes the process exothermic in air. At the end of this step the metastable acetonedicarboxylate complex was identified as the product. By isothermal heating of anhydrous nickel iron citrate in air around 175°C for about 4 h, the isolated acetonedicarboxylate on analysis gave, Ni = 10.7%, Fe = 19.7%, acetonedicarboxylate complex = 66.2% which were comparable with the calculated values, Ni = 9.4%, Fe = 17.9%, acetonedicarboxylate complex = 69.2%. Evolved gas analysis and TG weight loss indicates that 8 mol of CO gas was evolved. The acetonedicarboxylate was found to be X-ray amorphous and the varying weight loss occurs because of the metastable nature of the complex.

3.4. *Decomposition of acetonedicarboxylate complex*

The acetonedicarboxylate complex started decomposing at around 200°C in air and the decomposition was complete at around 320°C. At this stage the observed weight loss of 45.9% was found to be less than the calculated values of 47.0%. This may be due to the adsorption of extra CO_2 gas in the ultrafine $NiFe_2O_4$ particles which have a very large surface area of 120.0 $m^2\ g^{-1}$. At this stage decomposition is a complex process which involves decarboxylation (i.e. evolution of CO_2) and the acetone molecules formed. The evolution of acetone was confirmed by heating the residue $Ni_3Fe_6O_4(C_6H_6O_7)_8$ in a closed, hard-glass tube and condensing the evolved acetone in ice cold $CDCl_3$. The NMR spectrum in Fig. 3 clearly indicates the acetone proton peak at $\delta = 2.2$ ppm.

This means that when the precursor is decomposed at a higher temperature, above 200°C, the citrate precursor structure collapses and the formation of $NiFe_2O_4$ occurs with the evolution of acetone and CO_2 gas. The residue at this stage has a structure corresponding to nickel ferrite with trapped CO_2 gas; $Ni_3Fe_6O_{12}(CO_2)_3$ because of its fine particle nature has a large surface area. It is surprising that the decomposition does not go through the formation of complex carbonates, as has been reported in the literature [16–19], and it is also unusual that the formation of nickel ferrite occurs at a much lower temperature, i.e. 250°C. This residue dissolves in conc. HCl and black particles of carbon were not observed in the solution. The residue, $Ni_3Fe_6O_{12}(CO_2)_3$, is X-ray amorphous and becomes crystalline above 280°C. Heat treatment beyond 250°C over two days yields the stoichiometric $NiFe_2O_4$, the total weight loss being 6.5%. Isothermal heating of the citrate precursor around 280°C and above for 48 h yields a residue of the above constant composition, $NiFe_2O_4$, with a total weight loss of 68.1% compared with the 68.08% which results from the above calculations (Table 2). Chemical analysis of the residue, $Ni_3Fe_6O_{12}(CO_2)_3$, gave the observed values, Ni = 22.6%, Fe = 41.2%, compared with the theoretical values, Ni = 21.1%, Fe = 40.1%.

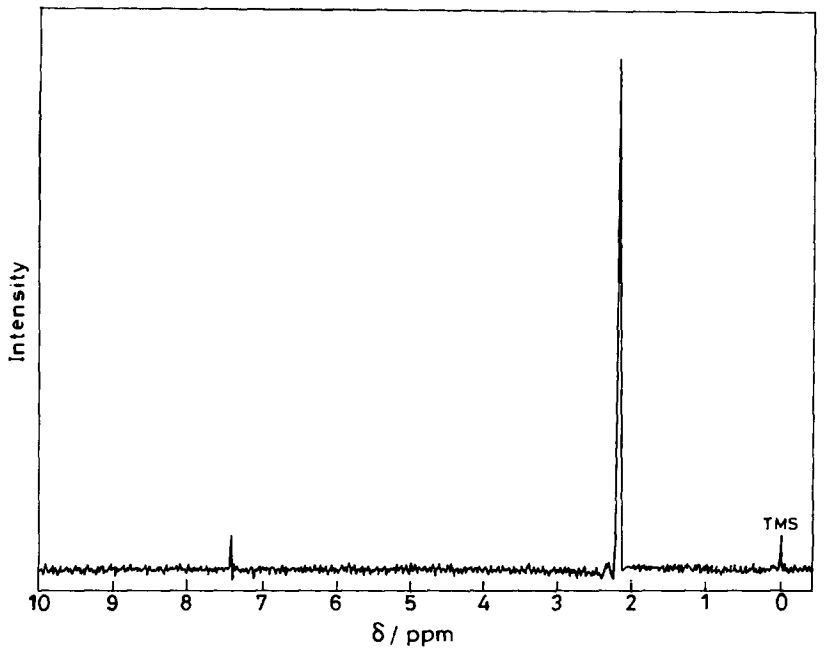

Fig. 3. NMR spectrum of acetone evolved during decomposition of acetonedicarboxylate complex.

However, the decomposition rate was found to be faster when the heating rate was $10^{\circ}\,min^{-1}$ (Fig. 2) which shows the decomposition of anhydrous nickel iron citrate precursor is a single step exothermic process leading to the formation of amorphous $Ni_3Fe_6O_{12}(CO_2)_7$ with the evolution of CO, CO_2 and acetone simultaneously. The decomposition temperature range is 160 to 200°C with the peak temperature at 180°C. The weight loss is 49.3% which is comparable with the static weight loss of 49.1% for the evolved gases. The adsorption of CO_2 gas is much larger in the residue, $Ni_3Fe_6O_{12}(CO_2)_7$, because of the fine particle nature and high porosity.

3.5. X-ray diffraction and IR spectral studies of the citrate precursor decomposition

Fig. 4 shows XRD pattern for the formation of intermediates and the spinel phase at various temperatures. The formation of pure single-phase $NiFe_2O_4$ occurs at around 250°C. Below 280°C, the $NiFe_2O_4$ phase is X-ray amorphous and crystallises completely above this temperature. The assignment of the IR bands is shown in Table 1 for the intermediates and the pure spinel phase. The absorption of citrate precursor occurs at 3429 (br), 2900 (w), 1700 (sh), 1570 (vs), 1400 (vs), 1270 (w) and 1080 (w) cm^{-1}. The 1700 (sh) and 1080 (w) cm^{-1} absorption bands disappear above 160°C retaining carboxylate absorption at 1570 and 1400 cm^{-1} [19]. This shows that the basic structure of the citrate breaks down by 160°C with the evolution of CO gas. The broad

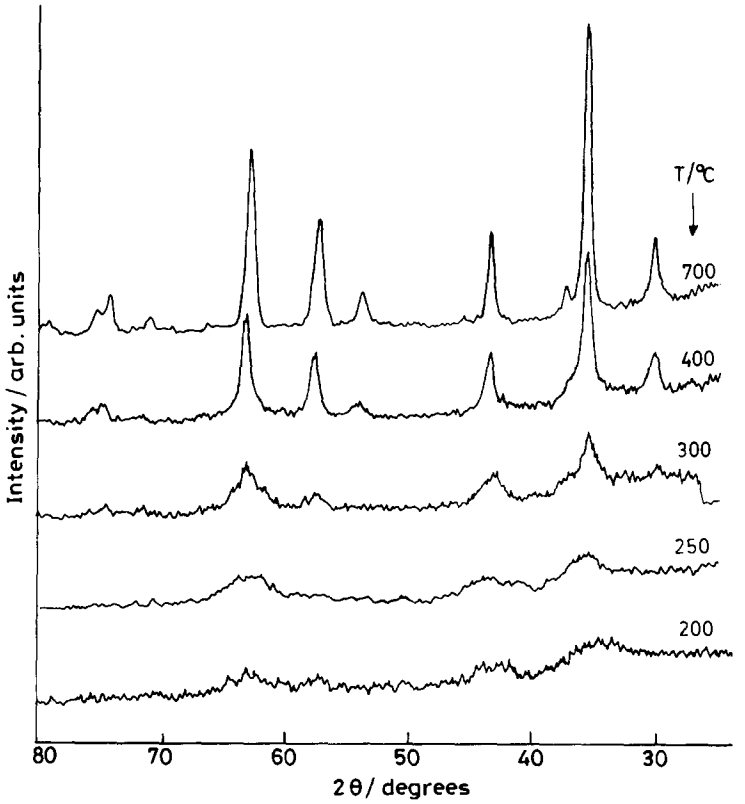

Fig. 4. X-ray diffraction patterns of decomposed products at various temperatures.

absorptions bands at 1570 cm^{-1} and 1400 cm^{-1} disappear above 200°C on longer heat treatment for 10 days. The IR spectrum at 280°C and above shows bands at 587 and 397 cm^{-1} which correspond to spinel phase formation; a sharp band at 2320 cm^{-1} must be due to the asymmetric stretching mode of free CO_2. The sharp absorption at 587 and 396 cm^{-1} is due to the lattice absorption of two NiO_4 and one FeO_4 group of tetrahedral symmetry in $NiFe_2O_4$ [20]. The increase in the intensity of these bands with heat treatment temperature above 320°C is understood in terms of the manifestation of crystalline $NiFe_2O_4$.

4. Discussion

The literature contains scanty information on the use of citrate complexes for ferrite formation; however thermal decomposition studies of citrate complexes for the formation of garnets [7,21], $LaCrO_3$ [22], $LaFeO_3$ [15], $LaCoO_3$, $LaCrO_3$, $SrCoO_3$, [23],

$BaTiO_3$ [17] have been reported. In general these studies show that impure citrate metal complex decomposition involves mainly three or four steps, which are as follows: removal of water of hydration and excess nitrate, and decomposition of the anhydrous citrate complex and free citric acid through intermediates such as aconitate, itaconate, itaconic anhydride and complex carbonates, leading to the respective oxides. In most of these cases citric acid and nitrates were present in considerable amounts [15,24] and thus the thermal decomposition studies are not comprehensive and remain inconclusive.

In the present studies neither free citric acid nor nitrates were present in the nickel iron citrate precursor and we have also successfully studied and reported the thermal decomposition of rare earth iron citrate [10]. Knowledge of citrate precursor structure will be very useful for predicting the number of citric acid molecules associated with the metal ions. However, little evidence is available in the literature concerning the possible structural arrangements of nickel iron citrate complex, although the citrate complexes of nickel and iron have been reported independently [25,26]. The extent of polymerization in the citrate complexes depends on pH [27,28] and in the lower pH ranges the extent of polymerization is not sufficient to form a network of solid structures; the nickel iron citrate precursor is, therefore, obtained in the pH range 1.25–2.00. It was also difficult to predict the binding metal ion sites with the citric acid; a plausible mechanism is, therefore, proposed on the basis of thermal analyses, chemical analyses and gas analyses, XRD, IR and NMR data. Nickel iron citrate hexahydrate precursor decomposes to the $NiFe_2O_4$ phase in air and the experimental results indicate the following scheme:

$$Ni_3Fe_6O_4(C_6H_6O_7)_8\cdot(n+6)H_2O \xrightarrow[<100^\circ C]{} Ni_3Fe_6O_4(C_6H_6O_7)_8\cdot 6H_2O + nH_2O \quad (1)$$

$$Ni_3Fe_6O_4(C_6H_6O_7)_8\cdot 6H_2O \xrightarrow[100-160^\circ C]{} Ni_3Fe_6O_4(C_6H_6O_7)_8 + 6H_2O \quad (2)$$

$$Ni_3Fe_6O_4(C_6H_6O_7)_8 \xrightarrow[160-200^\circ C]{} Ni_3Fe_6O_4(C_5H_6O_6)_8 + 8CO \quad (3)$$

$$Ni_3Fe_6O_4(C_5H_6O_6)_8 \xrightarrow[200-320^\circ C]{} Ni_3Fe_6O_{12}(CO_2)_3 + 8(CH_3COCH_3) + 13CO_2 \quad (4)$$

$$Ni_3Fe_6O_{12}(CO_2)_3 \xrightarrow[>320^\circ C]{} Ni_3Fe_6O_{12} + 3CO_2 \quad (5)$$

Nickel iron citrate hexahydrate complex was isolated by removing extra adsorbed water at around 100°C. The first step in the decomposition of the citrate precursor corresponds to the loss of coordinated water. The first and the second steps overlap and represent the major reactions in the thermal decomposition of anhydrous nickel iron citrate precursor. During the third step there is an evolution of CO gas. The residue after this decomposition step has only a metastable composition $Ni_3Fe_6O_4(C_5H_6O_6)_8$. In the fourth step complete internal conversion of carboxylate groups, methylene groups and hydroxyl groups takes place to form acetone and CO_2 gas which can be

observed by the disappearance of the absorption bands at 2900 cm^{-1} ($\nu_{sym.}$ CH), 1570 cm^{-1} ($\nu_{asym.}$ COO), 1400 cm^{-1} ($\nu_{sym.}$ COO), in the IR spectrum. The gases evolved, mainly CO_2 and acetone, were confirmed by the gas analysis data. Some CO_2 gas is adsorbed by the $NiFe_2O_4$ lattice because of its large surface area; it can be seen from the 2320 cm^{-1} absorption in the IR spectrum of residue, $Ni_3Fe_6O_{12}(CO_2)_3$. It was also mentioned earlier that the steps 2 and 3 occur as a single process between 160 and 200°C. When the decomposition is faster (i.e. heating rate 10° min^{-1}), the formation of $NiFe_2O_4$ phase is observed at a much lower temperature, i.e. around 200°C, with the simultaneous evolution of CO, CO_2 gases and acetone. The actual reactions appear to be simpler in the second and third steps unlike the reactions proceeding through aconitate complex formation by analogy with the thermal decomposition of the barium titanyl citrate complex [17]. This compound, $Ni_3Fe_6O_{12}(CO_2)_3$ was found to be X-ray amorphous and the adsorbed CO_2 gas disappears only on heating to around 250°C for more than 2 days. It is surprising that the decomposition does not proceed through the formation of complex carbonates as was reported in the literature [17] and, unusually, the formation of nickel ferrite occurs at a much lower temperature, i.e., 250°C. Finally, the crystallisation of this amorphous phase takes place above 280°C which is confirmed by the XRD pattern of the $NiFe_2O_4$ phase, (Fig. 4). The crystallised $NiFe_2O_4$ has a particle size of about 5.93 nm from the X-ray line-width measurement using the Scherrer method [29]. The surface area of crystallised $NiFe_2O_4$, measured by the BET method, was found to be 120.0 m^2 g^{-1}.

5. Conclusions

The synthesis of amorphous and crystalline $NiFe_2O_4$ ferrites by the citrate precursor method was investigated and the mechanism of thermal decomposition was examined in detail. The nickel iron citrate precursor was found to have the formula $Ni_3Fe_6O_4(C_6H_6O_7)_8 \cdot 6H_2O$; it was decomposed in a static air atmosphere resulting in the growth of pure and stoichiometric $NiFe_2O_4$ phase. Thermal decomposition of the citrate precursor consists of three major steps: dehydration, formation of acetonedicarboxylate complex and a decarboxylation process associated with the simultaneous evolution of acetone, yielding amorphous $Ni_3Fe_6O_{12}(CO_2)_3$ above 200°C. The high decomposition rate, low decomposition temperature and large amount of gases (i.e. CO, CO_2 and acetone) evolved results in the formation of ultrafine $NiFe_2O_4$ with a crystallite size of 5.93 nm which is evident from the measured surface area of 120.0 m^2 g^{-1}. Overall the formation of X-ray crystalline $NiFe_2O_4$ occurs at a relatively very low temperature i.e. above 250°C.

Acknowledgements

We acknowledge financial assistance during this investigation by the Department of Science & Technology, New Delhi. We are sincerely grateful to Professor U.C. Agarawala for fruitful discussions.

Reference

[1] T. Pannaparayil, R. Marande, S. Komarneni and S.G. Sankar, J. Appl. Phys., 64 (1988) 5641
[2] A. Goldman, in L. Levenson (Ed.) Electronic Ceramics, Marcel Dekker, New York, 1988, p. 170.
[3] S. Komarneni, E. Fregeau, E. Breval and R. Roy, J. Am. Ceram. Soc. Commun., 71 (1988) C-26.
[4] A.H. Morrish and K. Haneda, J. Appl. Phys., 52 (1981) 2696.
[5] D.W. Johnson, Jr., Am. Ceram. Soc. Bull., 60 (1981) 221, 243.
[6] C.H. Marcilly, P. Courty and B. Delmon, J. Am. Ceram. Soc., 53 (1970) 56.
[7] Ph. Courty, H. Ajot, Ch. Marcilly and B. Delmon, Powder Technology, 7 (1973) 21.
[8] A. Clearfield, A.M. Gadalla, W.H. Marlow and J.W. Livingston, J. Am. Ceram. Soc., 72 (1989) 1789.
[9] V.K. Sankaranarayanan and N.S. Gajbhiye, Thermochim. Acta, 153 (1989) 337.
[10] V.K. Sankaranarayanan and N.S. Gajbhiye, J. Am. Ceram. Soc., 73 (1990) 1301.
[11] A.I. Vogel, Text Book of Quantitative Inorganic Analysis, ELBS, England, 1986, p. 678.
[12] A.I. Vogel, Text Book of Quantitative Inorganic Analysis, ELBS, England, 1986, p. 466
[13] O.N. Karpov, Tr. Vses Nauchn.-Issled Inst. Khim. Reaktivov, 25 (1963) 334.
[14] C.J. Pouchart (Ed.) The Aldrich Library of NMR Spectra, Edition 11, Vol. 1, No 4580.
[15] H.M. Zhang, Y. Teraoka and N. Yamazoe, Chem. Lett., 4 (1987) 665.
[16] H.S. Gopalakrishnamurthy, M. Subbarao and T.R. Narayanan Kutty, J. Inorg. Nucl. Chem. 37 (1975) 891.
[17] D. Hennings and W. Mayr, J. Solid State Chem., 26 (1978) 329.
[18] N.S. Gajbhiye, U. Bhattacharya, V.S. Darshane, Thermochim. Acta, submitted for publication.
[19] R. Nakamoto, Infrared and Raman Spectra of Inorganic and Coordination Compounds, John Wiley, New York, 1978.
[20] R.D. Waldron, Phys. Rev., 99 (1955) 1727.
[21] Th. J.A. Popma and A.M Van Diepen, Mater. Res. Bull., 9 (1974) 111.
[22] J.M.D. Tascon, S. Mendioroz and L. Gonzalez Tejuca, Z. Phys. Chem (N.F.), 124 (1981) 109.
[23] D.J. Anderton and F.R. Sale, Powder Metall., 22 (1979) 14.
[24] B. Delmon and J. Droguest, in W.E. Kuhn and J. Ehretsmann (Ed.), Fine particles, Electrochemical Society, Princeton, NJ, 1974, p. 242.
[25] R.K. Patnaik and S. Pani, J. Ind. Chem. Soc., 34 (1957) 619.
[26] E. Belloni Milan, Crazz Chimital, 50 (1920) 159.
[27] C.J. Brinker and G.W. Scherer, J. Non-cryst. Solids, 70 (1985) 301.
[28] C.J. Brinker and G.W. Scherer, in L.L. Hench and D.R. Ulrich (Eds.), Ultrastructure processing of Ceramics, Glass and Composites, John Wiley, New York, 1985, p. 43.
[29] B.D. Cullity, Elements of X-ray diffraction, Addison Wesley, USA, 1978, p. 284.